# Pollution Characteristics and Human Health Risk of Potentially Toxic Elements Associated with Deposited Dust of Sporting Walkways During Physical Activity

Alghamdi, Mansour A.; Hassan, Salwa K.; Al Sharif, Marwan Y.; Khoder, Mamdouh I.; Harrison, Roy

[Link to publication on Research at Birmingham portal](#)

# Pollution characteristics and human health risk of potentially toxic elements associated with deposited dust of sporting walkways during physical activity

Mansour A. Alghamdi [a], Salwa K. Hassan [b], Marwan Y. Al Sharif [a], Mamdouh I. Khoder [b], Roy M. Harrison [a,c,*]

[a] *Department of Environmental Sciences, Faculty of Meteorology Environment and Arid Land Agriculture, King Abdulaziz University, P.O. Box 80208, Jeddah, 21589, Saudi Arabia*
[b] *Air Pollution Research Department, Environment and Climate Change Institute, National Research Centre, El Behooth Str., Dokki, Giza, 12622, Egypt*
[c] *School of Geography Earth and Environmental Science, University of Birmingham, Edgbaston, Birmingham, B15 2TT, United Kingdom*

## ABSTRACT

Sporting walkways are planned features designed to facilitate physical exercise in urban areas. Potentially toxic elements (PTEs) associated with deposited dust (DD) of urban sporting walkways (USWs), suburban sporting walkways (SSWs) and residential sporting walkways (RSWs) in Jeddah, Saudi Arabia, were measured and interpreted in relation to concentration, spatial distribution, pollution level and human health risk. The elemental concentrations followed a similar pattern, but were generally lower than those in road dust. Pb, Zn, Cu, Cd, and As had elevated Crustal Enrichment Factors (>10), ranging up to 185 for Cd. Except for Fe, $\sum$PTE concentrations were in the following order: USWs (1431 mg/kg) > SSWs (1073 mg/kg) > RSWs (892 mg/kg). Based on the spatial pattern and enrichment factor, and ecological risk values, sporting walkways (SWs) had moderate to heavy pollution levels of Cd, As, Pb, Zn and Cu, and heavy to extreme pollution level of Cd in USWs. Cd presented a high ecological risk, accounting for 85% of the summed ecological risk indices of the elements with elevated concentration. Carcinogenic and non-carcinogenic risks for children and adults follow the order: USWs > SSWs > RSWs. Ingestion was the main pathway for carcinogenic and non-carcinogenic risks, well exceeding that for the dermal and inhalation pathway. Most risks to human health were generally within the acceptable range, although risks to children were generally higher than those to adults, by a factor of 5.5 for non-carcinogenic risk. Incremental Lifetime Cancer Risks for individual elements did not exceed $10^{-4}$ for any element.

## 1. Introduction

Deposited dust (DD) in urban areas is well known to be enriched in trace elements derived from road traffic and other local and long-range sources such as industry (Yang et al., 2020). Major contributions arise from automotive brake and tyre wear, and abrasion of road surface materials. Deposited dusts can be either washed from the road surface by rainfall, or resuspended into the atmosphere, leading to dispersion of the dust, and potential exposure of the local population through inhalation, ingestion, and generally as a minor pathway, skin absorption.

Deposited dusts contain a diverse range of both inorganic and organic contaminants arising from natural and anthropogenic sources. The elevated level of potentially toxic elements (PTEs) in the different environmental media is a significant concern, particularly for metals including Hg, Ni, Cu, Pb, Cd, Zn, Cr, As, V, and Mn, since they are non-degradable and may have harmful effects on human health (Nematollahi et al., 2021; Wang et al., 2020a; Adimalla and Wang, 2018; Hassan 2018). The health risks of PTEs are dependent upon toxicity, including carcinogenicity, and potential for exposure (Agency for Toxic Substances and Disease Registry, 2019; Rahman and Singh, 2019;

---

Antoniadis et al., 2019). Some are cumulative toxins (e.g. Pb and Cd) (Mohammadi et al., 2019; Dytłow and Górka-Kostrubiec 2021; Osorio-Martinez et al., 2021). Consequently, assessment of the environmental exposures and health risks of PTEs is of considerable significance.

Increased urbanization and industrialization processes that are a consequence of development policies in various countries of the world have led to an increase in the concentrations of PTEs in environmental media such as water, air, soil, dust, etc. (Pragg and Mohammed, 2019). Anthropogenic sources of PTEs in the urban environment are vehicular emissions, urban construction, combustion, pavement surfaces, domestic waste and industrial and mining emissions, whereas natural sources mostly involve rock and soil weathering, and subsequent atmospheric deposition (Cowan et al., 2021; Men et al., 2020; Kusin et al., 2018; Shaltout et al., 2019, 2020). The impact of rapid industrialization and urbanization can influence the characteristics and sources of urban traffic emissions and industrial pollution (Cui et al., 2020; Wang et al., 2020b); since both are major factors contributing to PTE pollution (Hou et al., 2019; Kara, 2020).

Regular physical activity, such as walking, cycling, and running, have various physiological benefits and improve well-being. During these activities, which often occur outdoors, the human ventilation rate and hence the volume of air entering the body are significantly increased. As a result, human inhalation exposures are increased during exercise (Flouris, 2006; Pierson, 1989). Exposure to elevated levels of air pollutants for extended periods of time during vigorous exercise can lead to a decline in cardiovascular functions, altered hematological parameters, and increased levels of pollutants in the bloodstream in healthy athletes (Carlisle and Sharp, 2001; McDonnell et al., 2012; Kargarfard et al., 2015).

In order to increase the opportunities for physical exercise, the authorities in Jeddah, Saudi Arabia, have installed sporting walkways (SW). The only previous study in walkways of Jeddah city was focused on the nature, origin and risk assessment of PAHs in dust deposited from ambient air on impervious surfaces on both sides of the sporting walkways (Alghamdi et al., 2021). However, there are no data concerning the concentrations, origin and human health risk from exposure to PTEs in SWs during physical activity. Therefore, this study is the first in-depth investigation of the pollution levels and adverse health effects of PTEs associated with DD on surfaces alongside SWs which lead to dust exposure during exercise on SWs. It also draws attention to the possible importance of land use planning in selecting the locations for physical activity facilities. The main objectives of the present study are to:1) determine and describe the distribution patterns of the dust-bound PTEs in the deposited dust on the SWs surfaces of Jeddah city; 2) assess the PTE contamination levels in deposited dust using contamination indices; and 3) evaluate the resulting possible human health risks from exposure to dust-bound PTEs, using the USEPA risk assessment models. Such models evaluate exposure concentrations, intakes for both adults and children by ingestion, inhalation and dermal exposures, and the associated level of risk. The results have utility well beyond the local context of Jeddah. Strategies for promotion of public health worldwide include increased exercise, which can most economically be achieved out of doors. Hence the initiative of the Saudi authorities in providing dedicated outdoor space for exercise is likely to be followed elsewhere, and this study examines aspects of the risks posed to individuals using the sporting walkways. The results are of utility in devising strategies which mitigate that risk.

## 2. Materials and methods

### 2.1. Study area

Jeddah city is located in the middle of the Red Sea eastern coast of Saudi Arabia (21.4858° N, 39.1925° E respectively) (Fig. 1) where the origin of the city dates back to nearly 3000 years (Azzam and Ali, 2019).
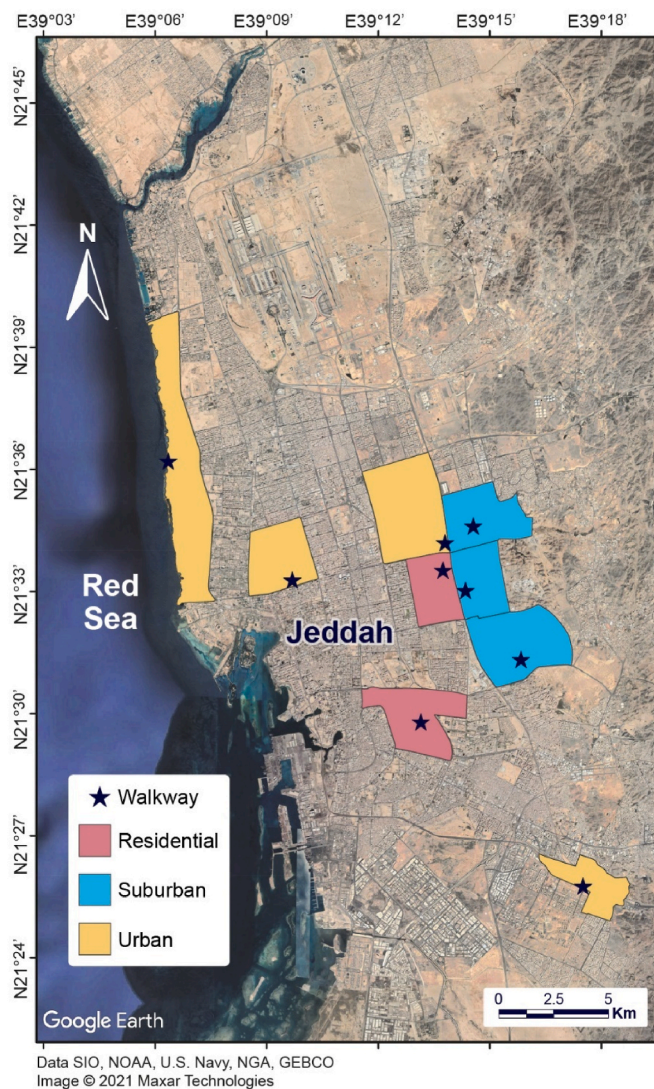


**Fig. 1.** Map of Jeddah city showing districts and the sporting walkways sampling sites.

Its urban area is approximately 1765 km$^2$, the total area is approximately 5460 km$^2$ (Amanah, 2022), and its population has nearly doubled since 1995 with steady yearly growth of about 3.5% to reach 4.0 million as estimated in 2016 (Abubakar and Aina, 2016).

Jeddah's climate is hot, humid in summer, mild and dry in winter with an average temperature that ranges from 28 °C in winter and can reach 40 °C in summer. The rainfall is irregular and infrequent with approximately 52 mm on average which occurs during winter and spring with frequent strong thunderstorms. The wind is dominantly from the northwest, and sandstorms are frequently blown into the city. Jeddah is considered the most important city on the eastern coast, and is the second largest of the country after the capital, Riyadh. The city has importance as a gateway to the holy city of Makkah Al Mukarramah through its seaport and airport, and accommodates many historical, industrial, commercial and tourist activities.

The city of Jeddah has contributed much to the implementation of the Kingdom's Vision, 2030, which stated in its social part: "Enhance people's walking habits" (Vision, 2016). Therefore, new public facilities including sporting walkways have been built during the past years in the city, and the number is increasing (Tiwari, 2022). Currently, the city houses 23 SWs that are encouraging a large number of townspeople of various ages to walk, jog or just relax in the open air, constructed to improve and support residents' wellbeing and health. SWs contain

particular areas for bicycling, exercise equipment, seats for the elderly, and special needs accessibility (SPA. Saudi Press Agency, 2020). SWs are characterized by the availability of public car parks, car parks for people with special needs, children's play areas, food trucks, etc. However, the majority of these walkways are surrounded by large automobile parking areas, located on busy roads, and in some instances are near to major intersections and highways. Photographs of a number of SWs appear in Fig. S1.

## 2.2. Sample collection strategy

During the period of mid-January to mid-February 2020 as described in our previous study (Alghamdi et al., 2021), the dust deposited from ambient air on different impervious surfaces like lampposts, seats, electric cabins and from windows and doors of public buildings located on both sides of the SWs were collected. The sampling sites were located on nine different SWs, at positions in Jeddah city displayed in Fig. 1. The SWs were located in urban, residential and suburban areas of Jeddah city. Twenty-seven DD samples were collected from these different SWs. At each walkway site, samples were collected by gentle sweeping, with new polyethylene brushes regularly pre-cleaned with deionized water to remove any contamination. The collected samples were put in airtight polyethylene bags, sealed, labelled and then transferred to the laboratory for the elemental analysis. Three DD samples, each amounting to 2–4 g, were collected from different areas from each SW. Any visible hair or coarse grit in the samples was removed before air-drying at room temperature. DD samples were then put in a desiccator to eliminate residual moisture and were homogenized. Then, they were kept in sealed polyethylene bags for elemental analysis.

## 2.3. Acid digestion and analysis

The glassware and filters utilized for digestion and analysis of the elements in the DD were acid washed with a dilute $HNO_3$ solution, rinsed with deionized water, and oven dried to prohibit contamination of samples during the extraction steps. The digestion procedure of DD samples for their elemental analysis was carried out according to USEPA protocol 3051A (USEPA, 2007). All chemicals used for sample digestion and analysis were obtained from the Merck Company. To determine the concentrations of eleven (11) PTEs in DD from SWs (Fe, Mn, Zn, Pb, Cd, V, Co, Ni, As, Cr, Cu), 0.3 g of each sample was weighed and transferred into a pre-cleaned conical flask of 50 ml volume. Then, ten (10) ml of aqua regia (HCl: $HNO_3$; 3:1 v/v) was added to the conical flask and allowed, in the fume hood, to digest overnight. After the overnight period, the samples were placed on a hotplate for 2 h at 90 °C until evaporated near to dryness. Thereafter, five (5) ml of deionized water were added to the samples and heated at 100 °C on the hotplate until close to dryness. Then, 25 ml of deionized water were added to the samples, cooled to room temperature, and filtered through Whatman filter paper (No. 42; pore size 2.5 μm). The digestates were stored at 4 °C in pre-cleaned polyethylene bottle until analysis by Inductively Coupled Plasma Optical Emission Spectrometry (ICP - OES 5100, Thermo Fisher Scientific, MA, USA).

## 2.4. Quality assurance and quality control (QA/QC)

QA/QC was carried out continuously and included dust digestion processes and analyses of field, laboratory and reagent blanks, analytical standards, ICP - OES 5100 calibration and detection limits in parallel with each ten (10) digested DD samples. Calibration curves for the target PTEs were prepared from stock standard PTE solutions. In order to evaluate any contamination, concentrations resulting from the laboratory blanks, HCl and $HNO_3$ acids and the deionized water using in the digestion process as well as filter blanks were determined by the same analytical procedures. No PTEs were detected. To assess the precision and accuracy of the ICP OES- 5100, standard solutions of PTEs were run

as a sample after analyzing each ten (10) digested DD samples. The limits of detection (LODs) for PTEs were determined from replicate measurements of low concentration samples and their standard deviations. LODs for measured PTEs were 105, 85.0, 101, 140, 130, 193, 192, 80.3, 60.0, 35.0, and 130 ng/g for Pb, Cr, Mn, Co, Ni, Cu, Zn, Cd, V, As, Fe, respectively. The relative standard deviation (RSD) estimated from the repeated measurements of the standards was used to determine the analytical precision of measured PTEs, and was below 2.6% for all elements. Extraction efficiencies were high, as established by analysis of SRM by this method in earlier work (Shabbaj et al., 2018).

## 2.5. Pollution characteristics

Contamination indices including enrichment factors (EFs), and potential ecological risk index (ERI) were used to assess the contamination levels of the PTEs associated with DD of the SWs.

### 2.5.1. Enrichment factors (EFs)

A common method to assess the degree of the anthropogenic influence upon trace element concentrations is the determination of the enrichment factors (EFs) for elements (Okedeyi et al., 2014; Li et al., 2017). EFs for PTEs in dust collected from SWs were calculated using equation (1):

$$EF = \frac{\left(C_n / C_{ref}\right)_{sample}}{\left(B_n / B_{ref}\right)_{background}} \quad (1)$$

where, $C_n$ and $B_n$ are the concentration of the target PTE in the DD sample and in background crustal material, respectively. $C_{ref}$ and $B_{ref}$ are the concentration of the reference element in the DD sample and background, respectively. Elements such as Ti, Fe, Al, Zr, and Mn, are commonly adopted as reference elements in the calculation of EFs for PTEs to distinguish their anthropogenic sources from naturally occurring material (Mediolla et al., 2008; Neto et al., 2006). In the present study, Fe was chosen as the reference element in the EF calculation, due to its high natural abundance, and relatively small influence of anthropogenic sources (Adimalla et al., 2019; Jiang et al., 2020). It is influenced by road traffic pollution, as it is present in brake wear particles (Harrison et al., 2021), but the background level in soils is so high that this has little influence upon road dust concentrations. Reference concentrations of iron and other elements were derived from two sources. The first was from the continental crust composition (Taylor, 1964; Taylor and McLennan, 1985; Bradl, 2005), and the second was the composition of a soil sampled from a rural site 60 km from Jeddah city (Hada Al Sham; Shabbaj et al., 2018). The degrees of PTE enrichment were classified into six pollution classes and are shown in Table S1.

### 2.5.2. Potential ecological risk assessment

Hakanson (1980) suggested the potential ecological risk index to evaluate the potential ecological risk for the environment (Perin et al., 1985; Yi et al., 2011). Nowadays, it is broadly used in contamination evaluations involving numerous elements (Mazurek et al., 2017; Odediran et al., 2021). The potential ecological risk factor (ER) for the given element was computed using the following equation (2) (Yuan et al., 2014).

$$ER = \frac{C_n}{C_b} \text{ X TRF} \quad (2)$$

where, $C_n$ is the concentration of the target elements in DD sample and $C_b$ is background (crustal) value of the target elements, and TRF is the toxic response factors for the elements which are: Cd (30), Cr (2), Cu (5), Pb (5), Zn (1), Ni (5), Mn (1) and As (10) (Hakanson 1980; Guo et al., 2010; Odediran et al., 2021). The Potential toxicity risk index (ERI), the summation of the individual ER values, was used to evaluate the contamination caused by all the measured PTEs simultaneously in each

DD sample. The formula for calculating ERI is shown in equation (3). The values of the ER and ERI grading standards are given in Table S1.

$$ERI = \sum EReach \tag{3}$$

### 2.6. Human health risk assessment

To assess the non-carcinogenic and carcinogenic health risks for both children and adults exposed to PTEs associated with DD of the SWs, the health risk assessment models depending on those developed by the USEPA (1989, 2011) were used. During physical activities at SWs in the open air the townspeople of various ages are exposed to PTEs via three base exposure routes of direct hand-mouth ingestion, nasal-oral inhalation and dermal contact. For the PTEs in SW dust, the summation of the risks estimated from these three exposure routes gives the total non-carcinogenic or carcinogenic health risks for this element for those elements acting systemically, as opposed to acting on a single receptor organ (e.g. the lung).

Based on the models (Equations (4)–(6)) set by USEPA (1989, 2001) that were also utilized already in several studies (e,g. Duggal and Rani, 2018; Shahab et al., 2020; Siddiqui et al., 2020; Patel and Jain, 2022), the average daily dose (ADD) (mg kg$^{-1}$ day$^{-1}$) for children and adults exposed to PTEs in DD of SWs via ingestion (ADD$_{ing}$), inhalation (ADD$_{inh}$) and dermal (ADD$_{dermal}$) pathways was evaluated. The various exposure factors utilized to compute the ADD values are listed in Table S2, which also defines the terms in the equations (also below). The application of this method assumes that the dust is representative of dust exposures throughout the day, which is an obvious simplification. No allowance is made for higher inhalation rates during exercise, but to do so would overestimate daily average exposures. It should also be noted that the estimation of inhalation (equation (5)) includes the highly uncertain term, PEF, which quantifies the relationship between deposited dust and that aerosolized and hence available for inhalation. The models do not account for the bioaccessibility of the elements for absorption, and this was not measured.

$$ADD_{ing} = \frac{C \times IngR \times EF \times ED}{BW \times AT} \times 10^{-6} \tag{4}$$

$$ADD_{inh} = \frac{C \times InhR \times EF \times ED}{PEF \times BW \times AT} \tag{5}$$

$$ADD_{dermal} = \frac{C \times SA \times AF \times ABF \times EF \times ED}{BW \times AT} \times 10^{-6} \tag{6}$$

After computing the ADD, the potentially non-carcinogenic risks of PTEs in SWs dusts were evaluated by computing the hazard quotient (HQ) (equations (7)–(9)) and hazard index (HI) (equation (10)), while the incremental lifetime cancer risk (ILCR) and the cancer risks (CR) were estimated using equations (11)–(14) (USEPA, 1989; Chen et al., 2012; Al-Harbi et al., 2021).

$$HQ_{ing} = \frac{ADD_{ing}}{R_fD} \tag{7}$$

$$HQ_{inh} = \frac{ADD_{inh}}{R_fD} \tag{8}$$

$$HQ_{dermal} = \frac{ADD_{dermal}}{R_fD} \tag{9}$$

$$Hazard\ index\ (HI) = HQ_{ing.} + HQ_{inh.} + HQ_{dermal} \tag{10}$$

$$ILCR_{ing} = \frac{C \times \left\{ CSF_{ingestion} \times \sqrt[3]{\left(\frac{BW}{70}\right)} \right\} \times IngR \times EF \times ED}{BW \times AT \times 10^6} \tag{11}$$

$$ILCR_{inh} = \frac{C \times \left\{ CSF_{inhalation} \times \sqrt[3]{\left(\frac{BW}{70}\right)} \right\} \times InhR \times EF \times ED}{BW \times AT \times PEF} \tag{12}$$

$$ILCR_{dermal} = \frac{C \times \left\{ CSF_{dermal} \times \sqrt[3]{\left(\frac{BW}{70}\right)} \right\} \times SA \times AF \times ABF \times EF \times ED}{BW \times AT \times 10^6} \tag{13}$$

$$Carcinogenic\ risk\ (CR) = ILCR_{ingestion} + ILCR_{inhalation} + ILCR_{dermal} \tag{14}$$

where: R$_f$D is the reference dose in mg kg$^{-1}$ day$^{-1}$ (USEPA, 1993), an assessment of dose giving the highest tolerable risk to humans via daily exposure by considering a sensitive group (children) during a lifetime; HQ$_i$ is the hazard quotient for single route; HI is the hazards index, non-carcinogenic risk from the different routes, and equal to the sum of HQ$_i$ for different exposure routes. the ILCR$_{ing}$ is the incremental lifetime cancer risk via ingestion, ILCR$_{inh}$ is the incremental lifetime cancer risk via inhalation, ILCR$_{dermal}$ is the incremental lifetime cancer risk via dermal contact. C the concentrations of the PTEs (mg kg$^{-1}$) in DD of SWs, CSF is the carcinogenic slope factor, BW is the body weight (kg), AT is the average life span (years), EF is the exposure frequency (day/year), ED is the exposure duration (years), InhR is the inhalation rate (m$^3$/day), IngR is the ingestion rate (mg/day), SA is the dermal surface exposure (cm$^2$), AF is the dermal adherence factor (mg/cm$^2$/h), ABF is the dermal absorption factor and PEF is the particle emission factor (m$^3$/kg). PEF is the particle emission factor (m$^3$/kg) describing aerosolization of the dust. The complete information regarding the values of exposure factors for children and adults used is listed in Table S2.

There is insignificant non-carcinogenic risk when HQ and HI ≤ 1, whereas the probability that non-carcinogenic risk occurs increases as HQ and HI rise beyond 1 (Zhang et al., 2019; USEPA, 2001, 2011). Likewise, ILCR and CR values below $1 \times 10^{-4}$ can be regarded as acceptable or tolerable levels, values above $1 \times 10^{-4}$ are widely considered to be unacceptable (potentially high risk), values below $1 \times 10^{-6}$ are generally taken as indicative of no significant health hazard (Gope et al., 2018; Men et al., 2018; USEPA, 1989, 2011; Islam et al., 2020).

### 3. Results and discussion

#### 3.1. Characteristics of PTEs in sporting walkways dust

##### 3.1.1. Concentration of PTEs in sporting walkways dust

Average concentrations of the individual PTE (11 elements) concentrations measured in DD of the different SWs of Jeddah are summarized in Table 1. The PTE concentrations in descending order were Fe > Mn > Zn > Pb > Cu > V > Cr > Ni > As > Co and Cd, accounting 90.18. 3.66, 3.06, 0.84, 0.83, 0.48, 0.39, 0.31, 0.13, 0.07 and 0.04% of the total PTEs concentrations, respectively. This PTEs pattern in DD of the SWs was similar to those found in classroom and street dusts of Jeddah city (Shabbaj et al., 2018; Alghamdi et al., 2019). The arithmetic

**Table 1**
Spatial variations of average PTEs concentrations in sporting walkways dust according to their function areas.

| | RSW | SSW | USW |
|---|---|---|---|
| Fe | 11,820 | 11,230 | 10,310 |
| Mn | 377 | 410 | 505 |
| Zn | 262 | 333 | 456 |
| Pb | 67.3 | 89.5 | 128 |
| Cd | 3.6 | 4.8 | 6.8 |
| V | 40.1 | 51.8 | 73.5 |
| Co | 5.8 | 7.6 | 10.5 |
| Ni | 25.7 | 33.1 | 46.3 |
| As | 10.4 | 13.9 | 19.8 |
| Cr | 32.6 | 41.8 | 59.3 |
| Cu | 67.8 | 88.2 | 127 |

mean concentration values were 10,950, 445, 372, 102, 5.4, 58.8, 8.5, 37.3, 15.8, 47.6, 101 mg/kg for Fe, Mn, Zn, Pb, Cd, V, Co, Ni, As, Cr and Cu, respectively. The PTE concentrations in DD of different SWs exceeded the background (crustal) values (Taylor, 1964; Taylor and McLennan, 1985; Bradl, 2005) only for Zn, Pb, Cd, As and Cu. Their mean concentration levels were 5.31, 8.13, 26.98, 8.75 and 1.83-fold higher than those in the background, respectively, indicating that these PTEs in DD of the SWs were strongly affected by the anthropogenic sources (Kosheleva et al., 2018; Zhao et al., 2019; Odediran et al., 2021) and accumulated in varied degrees. This finding is in line with Li et al. (2013) who found that the concentration values of trace metals in urban street dusts of a metropolitan city in China were 13 times greater than the background values. The concentrations of Pb, Zn, and Cd in road dusts of Ibadan were higher than the background values by 12, 2.4 and 11 times, respectively (Odediran et al., 2021).

From the comparison of Pb, Cu, Mn, Zn, Co and Cd concentrations in SWs dust with values suggested as their maximum permissible concentrations (MPC): 100 for Pb, 100 for Cu, 1500 for Mn, 300 for Zn, 30 for Co, and 3 Cd mg/kg in soil (Kabata-Pendias, 2010), only Zn and Cd were higher than the MPC and consequently might pose appreciable human health threats (Bali and Sidhu, 2021). According to the classification of the coefficients of variation (CV = SD/mean value), CV values were <0.2 for low variability, $0.2 \leq CV < 0.5$ for moderate variability, $0.5 \leq CV < 1.0$ for high variability and $CV \geq 1.0$ for extremely high variability (Pan et al., 2017). Based on the values of minimum and maximum concentrations, standard deviation (SD) and CV (Table S3), a considerable range in PTE concentrations was noticed. The values of CV, except for Fe and Mn, reveal moderate variability in the PTE concentrations in the DD samples and refer to the observed influence of anthropogenic activities on their levels (Yu et al., 2021; Zhang et al., 2020; Chen et al., 2021). On the other hand, the lowest CV values for Fe and Mn indicated weak variation and steady distribution of Fe and Mn across the different SWs areas, suggesting they originated mainly from natural sources. The presence of only a small gradient in Fe concentrations with the highest in the residential samples (Table 1) justifies the use of Fe as a crustal reference element.

The analyzed DD samples in the present study were collected from the surfaces of the SWs, and are analogous to outdoor dustfall and street dusts in relation to their elemental composition and sources. Until now, although there are studies of PTEs in deposited dusts (e.g. Khodadadi et al., 2022; Long et al., 2021; Wang et al., 2021), there are presently no publications on concentrations of PTEs associated with DD of any SWs worldwide. Accordingly, the PTEs in DD of SWs of Jeddah city were compared with those found in dustfall and street dusts from different cities across the world (Table S4). The PTE concentrations in DD of Jeddah SWs were well within the range of those found in dusts of other cities of the world. This observed variations in the PTE concentrations among these cities around the world back up the concept that this pattern of PTE contamination can be associated with anthropogenic activities, like urbanization, traffic density, economic growth rate and the types of fuels used, in each city.

Fig. 2 shows a comparison of elemental concentrations in SW dust in comparison to that of road dust, as measured in Jeddah by Shabbaj et al. (2018), for the three types of location. The profiles look remarkably similar, with road dust concentrations slightly exceeding those in the SW dust. The data sets were evaluated using a Student's t-test and statistically significant (P < 0.001) differences were found between the mean concentration of all the individual PTEs in residential road dust and residential sporting walkways (except for Fe) and in suburban road dust and suburban sporting walkways (except for Fe and Mn). However, no significant differences were found between the mean concentrations of all the individual PTEs in urban road dust and urban sporting walkways dust. This is a clear indication that both are affected by similar sources, and that resuspended road dust may be a major contributor to dusts on the SW, which are often located close to roadways.
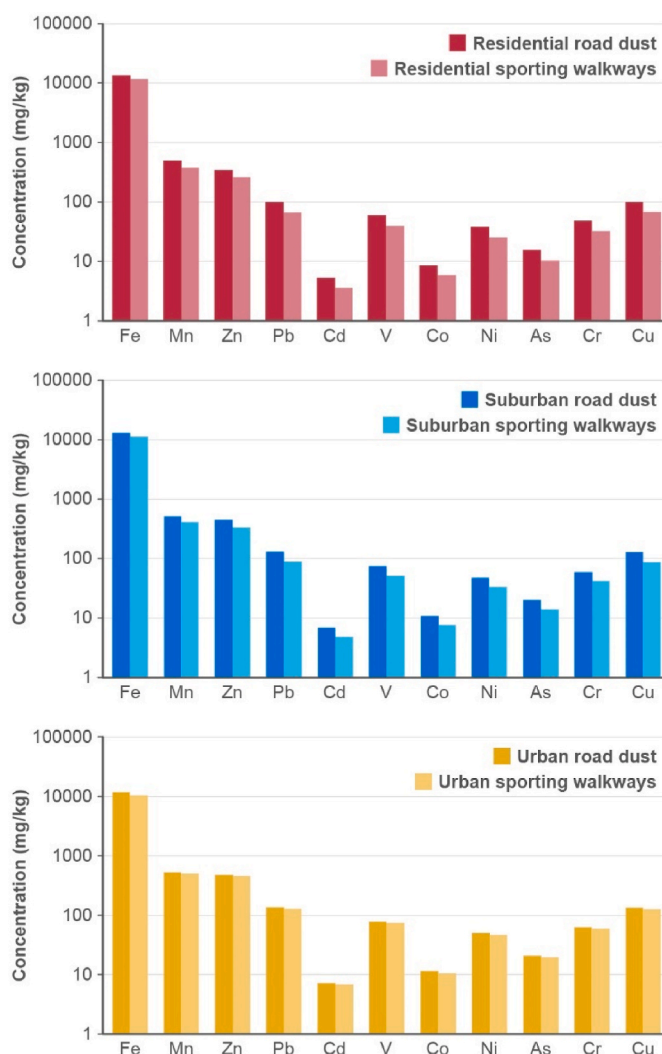


**Fig. 2.** Comparison of PTE in dust of sporting walkways with those found in road dusts in urban, suburban and residential areas. Road dust data from Shabbaj et al. (2018).

### 3.1.2. Spatial variations of PTEs concentrations in sporting walkways dust

Spatial variations of PTE concentrations based on their levels in DD of the different SWs and the classification of the SWs according to their functional areas in Jeddah are presented graphically in Fig. 3. Except for Fe, at all SWs, the highest individual and ∑PTEs concentrations were found at urban SWs (USWs) followed by suburban SWs (SSWs) and residential SWs (RSWs). Statistically significant (P < 0.001) differences were found between the mean concentration of all the individual PTEs in RSWs and USWs and in SSWs and USWs (except for Fe and Mn). Only the differences between the mean concentrations of Pb. V, Ni, As and Cu in RSWs and SSWs were statistically significant (p < 0.001). Moreover, the mean concentrations of the total ten PTEs (∑ Mn, Zn, Pb, Cd, V, Co, Ni, As, Cr and Cu) were in the following order: USWs (1431 mg/kg) > SSWs (1073 mg/kg) > RSWs (892 mg/kg), and only the differences between the mean concentrations of these total ten PTEs in USWs and SSWs and in USWs and RSWs were statistically significant (p < 0.001), indicating that the PTEs that accumulated in DD of SWs probably derived from anthropogenic activities. The higher levels of PTEs observed in USW dust may be attributable mainly to vehicular emissions from the heavy traffic along roads that run neighbouring the SW locations. Whereas the lowest PTEs found at RSWs are attributed to the relatively decrease in vehicular density with the absence of any emissions from the industrial activities. So, the pattern of spatial distribution of PTE concentrations in
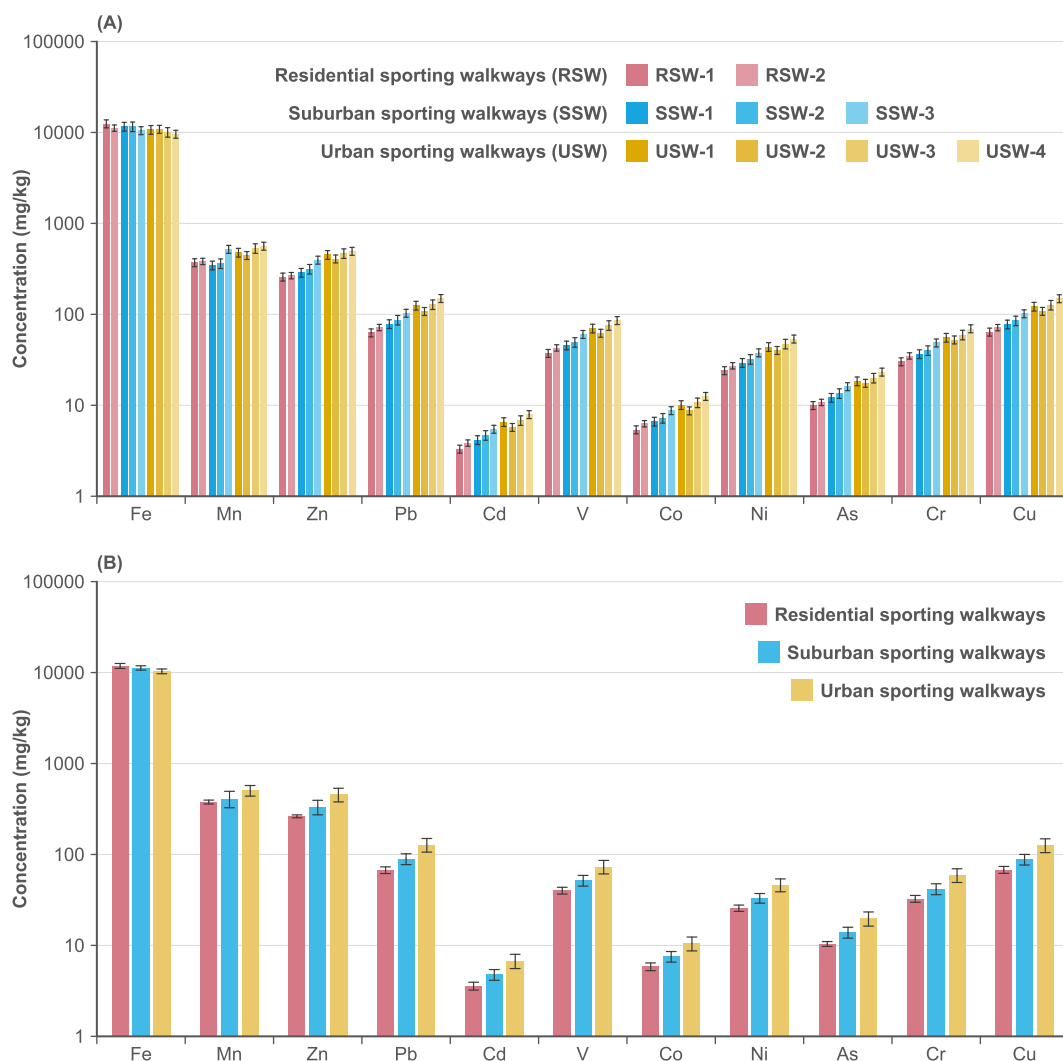
**Fig. 3.** Spatial variations of PTE concentrations: based on their concentrations in dust of different sporting walkways, and the classification of the sporting walkways according to their function areas; (A) all data, (B) averages for each area type and element.

the DD of Jeddah SWs was probably related to local anthropogenic sources.

Previous studies of PTEs in street and classroom dusts (Shabbaj et al., 2018; Alghamdi et al., 2019) showed spatial variations of PTE concentrations quite similar to that found in the SWs dust. Road traffic, the oil refinery and diesel/fuel oil combustion are the three main sources of pollution in Jeddah city (Alghamdi et al., 2015). Although the refinery and oil-burning desalination plant are the main point sources of pollution in Jeddah city, the measured concentration gradient of PTEs between urban, suburban and residential SWs is not consistent with a single point source, but is more probably explained by local street vehicular density.

If this work were to be taken further to examine contributions of individual sources (which was not one of our objectives), there are excellent examples in the literature of the use of geostatistical models and receptor models such as Positive Matrix Factorization to characterise the responsible sources (Wang et al., 2021; Jiang et al., 2021; Taiwo et al., 2020).

### 3.2. PTE pollution characteristics in sporting walkways dust

#### 3.2.1. Enrichment factor (EF)

The degree of enrichment of measured PTEs in DD of SWs in Jeddah varied from light to extreme enrichment with the classification criteria

of enrichment factors (EFs) (Table 2). Enrichment Factors were calculated both with respect to global average crustal composition and local background soil. Although the absolute values shown in Table 2 differ, the general pattern of values is similar for the two sets of reference data. The mean EF values of PTEs in DD of SWs of Jeddah estimated with respect to the global average crustal composition displayed the following increasing trend: Co < V < Mn < Cr < Ni < Cu < Zn < Pb < As < Cd (Table 2). EF values lower than 2 (light enrichment) were found for Mn, V, Ni, Co and Cr in RSWs, and for Co and V in SSWs, indicating that these PTEs originate largely from natural sources like crustal erosion and wind-blown soil minerals (Dytłow and Górka-Kostrubiec, 2021). EF values ranged from 2 to 5 were detected for Mn, Ni and Cr in SSWs, and for Mn, V, Co, Ni and Cr in USWs, suggesting they were moderately enriched. The refinery and desalination plant are expected to emit V and Ni from fuel oil combustion, but do not appear to be major contributors to contamination. EF values from 5 to 20 were found for Zn and Cu in RSWs and Cu in both SSWs and USWs, indicating they were significantly enriched, while values from 20 to 40 were recorded for Pb and As in RSWs, Zn, Pb, and As in SSWs and Zn in USWs, suggesting they were strongly enriched. Furthermore, the EF values for Cd in all SWs and Pb and As in USWs were higher than 40, indicating they were extremely enriched. The results of EF evaluation indicated that the five PTEs (Zn, Pb, Cd, As and Cu) in the DD of different SW areas had EF values higher than 5. These results were similar to those found in classroom and street

**Table 2**

Comparison of EFs of potentially toxic elements in sporting walkways dusts and road dusts of different functional areas based on global crustal average data and local background soil.

| | | Fe | Mn | Zn | Pb | Cd | V | Co | Ni | As | Cr | Cu |
|---|---|---|---|---|---|---|---|---|---|---|---|---|
| Residential sporting walkways | EF[a] | 1.00 | 1.89 | 17.85 | 25.63 | 85.15 | 1.41 | 1.11 | 1.63 | 27.46 | 1.55 | 5.87 |
| | EF[b] | 1.00 | 1.13 | 5.07 | 6.92 | 14.01 | 1.80 | 1.98 | 1.83 | 7.22 | 1.24 | 5.26 |
| Residential road dust | EF[a] | 1.00 | 2.17 | 20.56 | 33.27 | 110.36 | 1.84 | 1.44 | 2.12 | 36.33 | 2.00 | 7.61 |
| | EF[b] | 1.00 | 1.30 | 5.84 | 8.98 | 18.13 | 2.34 | 2.57 | 2.37 | 9.55 | 1.61 | 6.81 |
| Suburban sporting walkways | EF[a] | 1.00 | 2.16 | 23.84 | 35.86 | 119.73 | 1.92 | 1.51 | 2.21 | 38.76 | 2.10 | 8.04 |
| | EF[b] | 1.00 | 1.30 | 6.77 | 9.69 | 19.67 | 2.45 | 2.70 | 2.48 | 10.19 | 1.68 | 7.19 |
| Suburban road dust | EF[a] | 1.00 | 2.32 | 27.52 | 44.52 | 147.69 | 2.38 | 1.87 | 2.74 | 47.56 | 2.57 | 9.96 |
| | EF[b] | 1.00 | 1.39 | 7.81 | 12.02 | 24.26 | 3.03 | 3.33 | 3.07 | 12.50 | 2.06 | 8.91 |
| Urban sporting walkways | EF[a] | 1.00 | 2.90 | 35.56 | 55.85 | 184.82 | 2.97 | 2.30 | 3.37 | 60.07 | 3.24 | 12.56 |
| | EF[b] | 1.00 | 1.74 | 10.10 | 15.08 | 30.37 | 3.78 | 4.10 | 3.78 | 15.79 | 2.59 | 11.24 |
| Urban road dust | EF[a] | 1.00 | 2.61 | 31.93 | 51.66 | 171.38 | 2.76 | 2.17 | 3.18 | 55.20 | 2.98 | 11.56 |
| | EF[b] | 1.00 | 1.57 | 9.07 | 13.95 | 28.16 | 3.51 | 3.86 | 3.56 | 14.51 | 2.39 | 10.34 |

[a] based on global crustal average data.
[b] based on local background soil.

dust of Jeddah (Shabbaj et al., 2018; Alghamdi et al., 2019). Traffic emissions (brake dust, tire tread and, lubricating oil leakages) probably explain much of the Cu and Zn (Harrison et al., 2012). Incinerators are widely associated with the emission of Cd, Cu, Pb, As and Zn (Zhao et al., 2019, 2021; Patel and Jain, 2022; Mondal et al., 2020; Bourliva et al., 2018; Wang et al., 2019; Srithawirat and Latif, 2015; Al-Taani et al., 2019), and are a possible contributor. Corrosion processes under the influence of weather conditions may cause release of metals from street furniture such as street safety barriers, lamps and railings that often contain PTEs such as Zn, Cu, Cd and Cr (Bernardino et al., 2019; Novo et al., 2017; Trujillo-Gonzalez et al., 2016; Kamani et al., 2015), although corrosion in the dry atmosphere of Jeddah may be slower than in many other locations. Previous studies (Khodeir et al., 2012; Shabbaj et al., 2018; Alghamdi et al., 2019; Lim et al., 2018) have reported that, in despite of phase-out of Pb additive in gasoline in Saudi Arabia in 2001 (Aburas et al., 2011), the historical contamination of Pb can persist in the environment of Jeddah as a fraction of traffic-produced street dust with its long half-life and can also be resuspended (Nematollahi et al., 2021; Wang et al., 2020b). Similar processes have also been observed in London (Resongles et al., 2021), although brake dust may also be a source of lead.

*3.2.2. Ecological risk assessment*

The potential ecological risk factors (ER) of the measured eight PTEs (Cd, As, Pb, Cu, Zn, Ni, Cr, and Mn) in the DD of Jeddah SWs were calculated and are represented in Fig. 4. The pattern of ER for these PTEs follows similar distribution patterns in the different SW areas: ER values in descending order were Cd > As > Pb > Cu > Zn > Ni > Cr and Mn at all SWs, with highest values at USWs followed by SSWs and RSWs. The ER values were 537, 717, 1015 and 809 for Cd, 57.7, 77.4, 110, and 87.5 for As and 26.9, 35.8, 51 and 40.6 for Pb at RSWs, SSWs, USWs and All SWs, respectively. Based on the classification criteria of ER (Table S1), Pb showed lower ecological risk at RSWs and SSWs and moderate ecological risk at USWs. ER values of $40 \leq ER < 80$ were found for As at both RSWs and SSWs, indicating moderate risk to the ecological environment. As showed considerable ecological risk ($80 \leq ER < 160$) at USWs. On the other hand, Cd showed higher ER values ($ER \geq 320$) at all the different SWs, demonstrating high ecological risk for this element to the environment, representing 84.7% of the ecological risk indices (ERI) of the total PTEs. The results indicate that Cd is the major contributor to the ecological risk in DD of Jeddah SWs, and control of its emission is important to limit any threats to the ecosystem. Previous studies on the metals in road dust in Beijing and other areas reported that the higher ecological risk was associated with Cd (Men et al., 2018; Ni et al., 2018). Ecological risk indices (ERI) in this study were evaluated by summing the individual ER for the measured PTEs (Fig. 4). All SWs (RSWs, SSWs and USWs) showed ERI values higher than 600, meaning that these SWs were exposed to very high potential ecological risk. The highest ERI value (1199) was found in USWs, whereas the lowest value was in RSWs (634), attributed to the higher traffic density around the USWs. Kamani et al. (2017) reported that the highest ERI values were related to bad traffic jams in the centre of Tehran, Iran. In the present study, the ER and
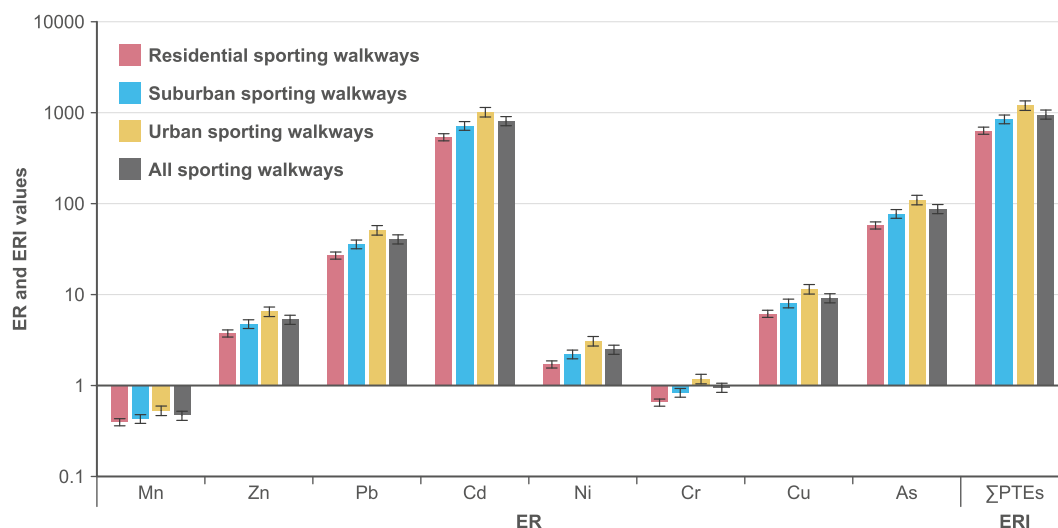


**Fig. 4.** Variation of potential ecological risks for PTEs in deposited dust of residential, suburban, urban and all sporting walkways.

ERI results are consistent with EF results.

### 3.3. Human health risk assessment

The carcinogenic and non-carcinogenic health risks for both children and adults were computed via three pathways (dermal, ingestion and inhalation), and then the hazard quotients (HQs: $HQ_{ing}$, $HQ_{inh}$ and $HQ_{dermal}$), hazard index (HI) and incremental lifetime cancer risk (ILCR) and cancer risk (CR) of PTEs in DD of SWs were evaluated.

#### 3.3.1. Non-carcinogenic risk

Based on the concentrations of PTEs in DD of different SWs, the $HQ_{ing}$, $HQ_{inh}$, $HQ_{dermal}$ and HI for both children and adults exposed to PTEs associated with DD of USWs, SSWs, RSWs and all SWs were calculated and are listed in Table S5. These are based upon the Reference Doses listed in Table S6. The values of HI for the individual PTEs and their sum, for children and adults at the different SWs based on their location were in the order of USWs > SSWs > RSWs. At all SW areas, the HQ values for the different exposure pathways of measured PTEs decreased in the following order: ingestion > dermal contact > inhalation. At all SW locations, the HI, $HQ_{ing}$ and $HQ_{inh}$ of children were higher than for adults in the different SWs, whereas $HQ_{dermal}$ for adults were higher than for children. The HI, $HQ_{ing}$ and $HQ_{inh}$ for children, respectively, were 5.5, 9.3, and 2.8 times than those for adults, whereas $HQ_{dermal}$ for adults was 2 times than that of children. The higher $HQ_{ing}$ for children than adults may be attributed to the raised inclination of children to ingestion dust-bound potentially toxic elements probably due to the habit of taking each thing into their mouth, indifference to cleanness, and playing in dusty surrounding settings (Habil et al., 2013; Latif et al., 2014). Similar results already have been reported in previous studies (Qadeera et al., 2020; Chen et al., 2017; Zheng et al., 2010).

The percentage risk contributions via $HQ_{ing}$, $HQ_{inh}$ and $HQ_{dermal}$ to the HI for children were 93.8, 2.47 and 3.74% (RSWs), 94.4, 1.93, and 3.65% (SWSs) and 94.96, 1.44, 3.60% (USWs) and 94.6, 1.7 and 3.6% (all SWs), respectively. Likewise, the risk contributions of $HQ_{ing}$, $HQ_{inh}$ and $HQ_{dermal}$ to the HI for adults were 54.1, 4.79 and 41.1 at RSWs, 55.4, 3.80 and 40.8% at SSWs, 56.4, 2.88 and 40.7% at USWs and 55.8, 3.5 and 40.8% at all SWs, respectively. Accordingly, ingestion was the main exposure pathway of PTEs associated with DD of the SWs in both adults and children, followed by dermal and inhalation pathways; similar trends were found in numerous previous studies (Chen et al., 2019; Ferreira-Baptista and De Miguel, 2005; Men et al., 2018; Shabbaj et al., 2018; Alghamdi et al., 2019).

HQs exceeding or equalling one (HQs ≥1) suggest unsafe risk (harmful health effects), whereas HQs lower than one (HQs <1) indicate an acceptable hazard level (USEPA, 2011). Based on the exposure to ∑PTE concentrations, only the values of $HQ_{ing}$ and HI for children were higher than the safe level (>1), they were 1.1, 1.45 and 2.03 for $HQ_{ing}$, 1.2, 1.5 and 2.1 for HI at RSWs, SSWs and USWs (Table S5), respectively. These results reveal that children faced more potential health risk and "an unacceptable hazard level" through ingestion of ∑PTEs in DD of SWs in Jeddah city. Regarding the individual PTE concentrations in DD particles collected from RSWs, SSWs, USWs and all SWs of Jeddah, $HQ_{ing}$, $HQ_{inh}$, $HQ_{dermal}$ and HI values for all measured PTEs were within the safe level (<1), with highest values for As, Pb, Cr and Mn at the different SWs (Table S5). Moreover, $HQ_{ing}$ and HI values for children only from exposure to As, Pb, Cr and Mn at the different SWs were above 0.1. The $HQ_{ing}$ and HI were also above 0.1 for adults exposed to V in SSWs and USWs. High levels of potentially toxic metals (PTMs) can cause severe developmental and neurological health impacts, particularly for children due to higher exposure rates of PTMs with regard to their body weight (Ali et al., 2017; Cheng and Hu, 2010; Li et al., 2014).

The percentage risk contribution of HI for each PTE to ∑HI for all PTEs in the different SWs indicated that As was the dominant contributor to non-cancer effects in the different SWs, and it represented 37.2% and 23.0% (RSWs), 38.8% and 24.4% (SSWs), 39.6% and 25.2%

(USWs), and 39.0% and 24.6% (all Jeddah SWs) of the total effects for children and adults, respectively. As a result, the probable non-carcinogenic risk from PTEs, especially for As, Pb, Cr and Mn, in dust of Jeddah SWs cannot be neglected, since any further increase in the anthropogenic activities may raise their contamination levels and hence health risk.

#### 3.3.2. Carcinogenic risk

Incremental lifetime cancer risk (ILCR) is used as an index to estimate the cancer risks after simultaneous exposure through three pathways (ingestion, inhalation, dermal). Among the measured eleven PTEs, ILCR for six PTEs (Cr, Ni, Cd, Pb, Co and As) were selected and considered to assess carcinogenic risk (Li et al., 2018) for children and adults, and are listed in Table S7. These are based upon cancer slope factors listed in Table S8; in the case of Co, these were available only for the inhalation exposure pathway. From the calculated ILCR ($ILC_{ing}$, $ILCR_{inh}$, $ILCR_{dermal}$) and total cancer risk (CR = ∑$ILCR_{ing}$ + $ILCR_{inh}$ + $ILCR_{dermal}$) for children and adults from the exposure to individual and ∑PTEs in DD of different SWs (Table S7), the sequence of cancer risks (ILCRs and CR) of the different areas was USWs > SSWs > RSWs. This difference in cancer risks among the three SW areas reflected the considerable effects of source emissions of PTEs on the health risk. Based on the exposure pathways, ILCR values for children and adults at various SWs decreased in the following order: ingestion > dermal contact > inhalation; a similar kind of trend was reported in previous studies (Duggal and Rani, 2018).

The contributions of $ILCR_{ing}$ to the CR were 73.3% and 58.5% (RSWs), 73.3% and 57.6% (SSWs) and 76.2% and 57.5% (USWs) for children and adults, respectively, indicating that ingestion is the main responsible pathway for CR in both children and adults. These results are in agreement with Odediran et al. (2021) who reported that $ILCR_{ing}$ represented 99.83% and 97.04% of CR for children and adults, respectively, from exposure to road dust. At each and all SWs (Table S7), the results for $ILCR_{ing}$, $ILCR_{inh}$, $ILCR_{dermal}$ and CR from exposure to the individual and ∑PTEs indicated that $ILCR_{ing}$ and CR were higher for children than adults and vice versa for $ILCR_{inh}$. On the other hand, there are no differences between the values of $ILCR_{dermal}$ for children and adults. The $ILCR_{ing}$ for children was 2.24–2.33 times than that for adults, whereas $ILCR_{inh}$ for adults was 1.41–1.45 that of children. Moreover, the CR for children were 1.85 (RSWs), 1.76 (SSWs) and 1.75 (USWs) times than that of adults, showing them to be the most at-risk group. This is in agreement with Ali et al. (2017) who found that health risks for children from exposure to heavy metals were higher by 1.9–15 times than that of adults. CR for the various PTEs in all SWs ranked the following order: Ni > Cr > As > Cd > Pb > Co. If incremental cancer risks of >$10^{-4}$ for a single element are taken as unacceptable, cancer risks, although not negligible, do not exceed this level.

### 3.4. Limitations of the study

The research is very much a preliminary scoping of possible risk associated with SW use. It is limited in terms of the number of SWs sampled, and the elements analyzed. PAH have been assessed in a parallel study (Alghamdi et al., 2021), but other organic compounds have not been assessed. A more comprehensive study would remedy these deficiencies, and with a larger dataset could apply geospatial techniques and receptor models to identify sources of contaminants, as reported by Wang et al. (2021), Jiang et al. (2021) and Taiwo et al. (2020).

## 4. Conclusions

This study has met its overall objectives. It has sampled dusts from a number of SWs across Jeddah representative of different areas of the city. The levels of contaminants have been established and compared with contaminant indices and used in an evaluation of risks to adults and children. Out of the eleven PTEs measured in DD collected from different

SWs in Jeddah, only the mean concentrations of Pb, Zn, Cu, Cd, and As were noticeably higher than the corresponding background values. Their concentration levels were 5.31, 8.13, 27.0, 8.75 and 1.83 fold higher than those in the background, respectively. The mean concentrations of the total ten PTEs ($\sum$Mn, Zn, Pb, Cd, V, Co, Ni, As, Cr and Cu) in DD were in the following order: USWs (1431 mg/kg) > SSWs (1073 mg/kg) > RSWs (892 mg/kg), indicating that this PTEs probably derived from anthropogenic activities, and their highest levels in USWs might be attributed mainly to the vehicular emissions from the heavy traffic density along roads that run adjacent to SW locations. This is supported by the very similar concentration profile of PTEs in road dust sampled in Jeddah (Shabbaj et al., 2018) to that from the SWs. EF estimates showed that Pb, As, Zn, and Cd varied from strongly enriched to extremely highly enriched, suggesting that these PTEs were very largely affected by anthropogenic sources. All SWs were exposed to very high potential ecological risk, with the highest ERI value in USWs attributable to the higher traffic density around the USWs. Cd is the major contributor to the ecological risk in DD of Jeddah SWs, representing 84.7% of the ecological risk indices (ERI) of the total PTEs, and control its emission is important to limit any threats to the ecosystem. ER and ERI results are consistent with the EF values, confirming that monitoring of the Zn, Pb, Cd, and As concentrations in DD of SWs is recommended to be continuously to be in place to safeguard ecosystem health.

The health risk model revealed that the hazard quotient (HQ) values for non-carcinogenic risk and incremental lifetime cancer (ILCR) values for carcinogenic risk followed the trend of ingestion > dermal contact > inhalation, indicating that the direct hand-to-mouth intake is the major significant route for both non-carcinogenic and carcinogenic risks from SWs dust. HQ, ILCR, Hazard index (HI), cancer risk (CR) for children were higher than that for adults, suggesting that children were more exposed to both non-cancer and cancer risks than adults during physical activities on SWs. The CR, HI, ILCR$_{ing}$ and HQ$_{ing}$ risks posed by $\sum$PTEs in children were higher at all SWs, confirming that children were more prone to both non-cancer and cancer risks during physical activities on SWs, as is typically the case. However, no significant cancer and non-cancer risks were observed from the dermal and inhalation pathways. The sequence of cancer and non-cancer risks of the different SWs based on their areas was USWs > SSWs > RSWs. Considering that SW use is likely to be for a few hours, at most, of the day, the risks associated with PTE exposure are unlikely to be large.

In general, this study showed the effect of pollution sources, particularly traffic emissions, on the spatial variations of pollution levels, and consequent ecological and human health risks arising from the exposure to PTEs associated with dust of Jeddah SWs. Therefore, the output of this study could serve as significant data for further evaluation of exposure and health risks for SWs in Saudi Arabian cities, and those in other countries that adopt SWs to encourage physical exercise. The data can also raise awareness amongst pertinent stakeholders regarding exposure during physical activities on SWs, and can help inform the processes for selecting the future locations of SWs. Significant findings include the close relationship between levels of dust on SWs and those in locally sampled soils. This gives a clear message in terms of selection of locations for developing SWs in order to minimise ecological and human health risk.

## Author contributions

Mansour A. Alghamdi. Salwa K. Hassan, Marwan Y. Al Sharif, Mamdouh I. Khoder, Roy M. Harrison, Conceptualization – MAA, MIK, Formal Analysis – MIK, RMH. Funding acquisition - MAA. Investigation – MYAS, MIK, SKH. Methodology – MAA, MIK, RMH. Project administration - MAA, Resources - MAA, Validation – MAA, MIK, RMH. Visualization – MAA, MIK. Writing – original draft – MAA, MIK. Writing – review & editing - RMH.

## Declaration of competing interest

The authors declare that they have no known competing financial interests or personal relationships that could have appeared to influence the work reported in this paper.

## Appendix A. Supplementary data

Supplementary data to this article can be found online at https://doi.org/10.1016/j.apr.2023.101649.

## References

Abubakar, I.R., Aina, Y.A., 2016. Achieving sustainable cities in Saudi Arabia: juggling the competing urbanization challenges. In: Population Growth and Rapid Urbanization in the Developing World. IGI Global, Hershey, PA, USA, pp. 42–63.

Aburas, H.M., Zytoon, M., Abdulsalam, M.I., 2011. Atmospheric lead in PM$_{2.5}$ after leaded gasoline phase-out in Jeddah City, Saudi Arabia. Clean: Soil, Air, Water 39, 711–719.

Adimalla, N., Qian, H., Wang, H., 2019. Assessment of heavy metal (HM) contamination in agricultural soil lands in northern Telangana, India: an approach of spatial distribution and multivariate statistical analysis. Environ. Monit. Assess. 191, 246.

Adimalla, N., Wang, H., 2018. Distribution, contamination, and health risk assessment of heavy metals in surface soils from northern Telangana, India. Arabian J. Geosci. 11, 684.

Agency for Toxic Substances and Disease Registry, 2019. Priority List of Hazardous Substances. https://www.atsdr.cdc.gov/spl/index.html#2019spl. (Accessed 29 December 2020). Accessed.

Alghamdi, M.A., Hassan, S.K, Al Sharif, M.Y., Khoder, M.I., Harrison, R.M., 2021. On the nature of polycyclic aromatic hydrocarbons associated with sporting walkways dust: concentrations, sources and relative health risk. Sci. Total Environ. 781, 146540.

Alghamdi, M.A., Hassan, S.K., Alzahrani, N.A., Almehmadi, F.M., Khoder, M.I., 2019. Risk assessment and implications of schoolchildren exposure to classroom heavy metals particles in Jeddah, Saudi Arabia. Int. J. Environ. Res. Publ. Health 16, 5017.

Alghamdi, M.A., Alam, M.S., Yin, J., Stark, C., Jang, E.-H., Harrison, R.M., Shamy, M., Khoder, M.I., Shabbaj II, 2015. Receptor modelling study of polycyclic aromatic hydrocarbonsin Jeddah. Saudi Arabia. Sci. Total Environ. 506–507, 401–408.

Al-Harbi, M., Alhajri, I., Whalen, J.K., 2021. Characteristics and health risk assessment of heavy metal contamination from dust collected on household HVAC air filters. Chemosphere 277, 130276.

Ali, M.U., Liu, G., Yousaf, B., Abbas, Q., Ullah, H., Munir, M.A.M., Fu, B., 2017. Pollution characteristics and human health risks of potentially (eco) toxic elements (PTEs) in road dust from metropolitan area of Hefei, China. Chemosphere 181, 111–121.

Al-Taani, A.A., Nazzal, Y., Howari, F.M., 2019. Assessment of heavy metals in roadside dust along the abu dhabi–al ain national highway, UAE. Environ. Earth Sci. 78, 411.

Amanah, 2022. Jeddah Municipality. https://www.jeddah.gov.sa/Jeddah/About/index.php. (Accessed 4 February 2022) (last Accessed.

Antoniadis, V., Shaheen, S.M., Levizou, E., Shahid, M., Niazi, N.K., Vithanage, ., Ok, Y.S., Bolan, N., Rinklebe, J., 2019. A critical prospective analysis of the potential toxicity of trace element regulation limits in soils worldwide: are they protective concerning health risk assessment? - a review. Environ. Int. 127, 819–847.

Azzam, A., Ali, A.B., 2019. Urban sprawl in wadi goss watershed (Jeddah city/western Saudi Arabia) and its impact on vulnerability and flood hazards. J. Geogr. Inf. Syst. 11, 371–388.

Bali, A.S., Sidhu, G.P.S., 2021. Heavy Metal Contamination Indices and Ecological Risk Assessment Index to Assess Metal Pollution Status in Different Soils, HMs in the Environment. Elsevier, pp. 87–98.

Bernardino, C.A., Mahler, C.F., Santelli, R.E., Freire, A.S., Braz, B.F., Novo, L.A., 2019. Metal accumulation in roadside soils of Rio de Janeiro, Brazil: impact of traffic volume, road age, and urbanization level. Environ. Monit. Assess. 191, 156.

Bourliva, A., Kantiranis, N., Papadopoulou, L., Aidona, E., Christophoridis, C., Kollias, P., Evgenakis, M., Fytianos, K., 2018. Seasonal and spatial variations of magnetic susceptibility and potentially toxic elements (PTEs) in road dusts of Thessaloniki city, Greece: a one- year monitoring period. Sci. Total Environ. 639, 417–427.

Bradl, H., 2005. Heavy Metals in the Environment. Interface (Heavy Metals in the Environment. Interface). 6. Science and Technology. Elsevier Ltd, London, p. 269.

Carlisle, A.J., Sharp, N.C.C., 2001. Exercise and outdoor ambient air pollution. Br. J. Sports Med. 35, 214–222.

Chen, L., Zhang, H., Ding, M., Devlin, A.T., Wang, P., Nie, M., Xie, K., 2021. Exploration of the variations and relationships between trace metal enrichment in dust and ecological risks associated with rapid urban expansion. Ecotoxicol. Environ. Saf. 212, 111944.

Chen, Q.-X., Huang, C.-L., Xiao, T., Yuan, Y., Mao, Q.-J., Tan, H.-P., 2019. Characterization of atmospheric aerosols and source apportionment analyses in urban Harbin, northeast China. Infrared Phys. Technol. 103, 103109.

Chen, X., Liu, M., Ma, J., Liu, X., Liu, D., Chen, Y., Li, Y., Qadeer, A., 2017. Health risk assessment of soil heavy metals in housing units built on brownfields in a city in China. J. Soils Sediments 17, 1741–1750.

Chen, X., Lu, X., Yang, G., 2012. Sources identification of heavy metals in urban topsoil from inside the Xi'an second ring road, NW China using multivariate statistical methods. Catena 98, 73–78.

Cheng, H., Hu, Y., 2010. Lead (Pb) isotopic fingerprinting and its applications in lead pollution studies in China: a review. Environ. Pollut. 158, 1134–1146.

Cowan, N., Blair, D., Malcolm, H., Graham, M., 2021. A survey of heavy metal contents of rural and urban road- side dusts: comparisons at low, medium and high traffic sites in Central Scotland. Environ. Sci. Pollut. Res. 28, 7365–7378.

Cui, X., Wang, X., Liu, B., 2020. The characteristics of heavy metal pollution in surface dust in Tangshan, a heavily industrialized city in North China, and an assessment of associated health risks. J. Geochem. Explor. 210, 106432.

Duggal, V., Rani, A., 2018. Carcinogenic and noncarcinogenic risk assessment of metals in groundwater via ingestion and dermal absorption pathways for children and adults in Malwa Region of Punjab. J. Geol. Soc. India 92, 187–194.

Dytłow, S., Gorka-Kostrubiec, B., 2021. Concentration of heavy metals in street dust: an implication of using different geochemical background data in estimating the level of heavy metal pollution. Environ. Geochem. Health 43, 521–535.

Ferreira-Baptista, L., De Miguel, E., 2005. Geochemistry and risk assessment of street dust in Luanda, Angola: a tropical urban environment. Atmos. Environ. 39, 4501–4512.

Flouris, A.D., 2006. Modelling atmospheric pollution during the games of the XXVIII Olympiad: effects on elite competitors. Int. J. Sports Med. 27, 137–142.

Gope, M., Masto, R.E., George, J., Balachandran, S., 2018. Tracing source, distribution and health risk of potentially harmful elements (PHEs) in street dust of Durgapur, India. Ecotoxicol. Environ. Saf. 154, 280–293.

Guo, W., Liu, X., Liu, Z., Li, G., 2010. Pollution and potential ecological risk evaluation of heavy metals in the sediments around Dongjiang Harbor, Tianjin. Proc. Environ. Sci. 2, 729–736.

Habil, M., Massey, D.D., Taneja, A., 2013. Exposure of children studying in schools of India to PM levels and metal contamination: sources and their identification. Air. Qual. Atmos Health 6, 575–587.

Hakanson, L., 1980. An ecological risk index for aquatic pollution control. A sedimentological approach. Water Res. 14, 975–1001.

Harrison, R.M., Jones, A., Gietl, J., Yin, J., Green, D., 2012. Estimation of the contribution of brake dust, tire wear and resuspension to nonexhaust traffic particles derived from atmospheric measurements. Environ. Sci. Technol. 46, 6523–6529.

Harrison, R.M., Allan, J., Carruthers, D., Heal, M.R., Lewis, A.C., Marner, B., Murrells, T., Williams, A., 2021. Non-exhaust vehicle emissions of particulate matter and VOC from road traffic: a review. Atmos. Environ. 262, 118592.

Hassan, S.K., 2018. Sources and cancer risk of heavy metals in total suspended particulate in some square areas of greater cairo, Egypt. Indian J. Environ. Protect. 38, 1041–1050.

Hou, S., Zheng, N., Tang, L., Ji, X., Li, Y., Hua, X., 2019. Pollution characteristics, sources, and health risk assessment of human exposure to Cu, Zn, Cd and Pb pollution in urban street dust across China between 2009 and 2018. Environ. Int. 128, 430–437.

Islam, A.R.M.T., Islam, H.M.T., Mia, M.U., Khan, R., Habib, M.A., Bodrud-Doza, M., Siddique, M.A.B., Chu, R., 2020. Co-distribution, possible origins, status and potential health risk of trace elements in surface water sources from six major river basin, Bangladesh. Chemosphere 249, 126180.

Jiang, H.-H., Cai, L.-M., Hu, G.-C., Wen, H.-H., Luo, J., Xu, H.-Q., Chen, L.-G., 2021. An integrated exploration on health risk assessment quantification of potentially hazardous elements in soils from the perspective of sources. Ecotoxicol. Environ. Saf. 208, 111489.

Jiang, H.-H., Cai, L.-M., Wen, H.-H., Hu, G.-C., Chen, L.-G., Luo, J., 2020. An integrated approach to quantifying ecological and human health risks from different sources of soil heavy metals. Sci. Total Environ. 701, 134466.

Kabata-Pendias, A., 2010. Trace Elements in Soils and Plants. CRC Press, Boca Raton, FL, USA.

Kamani, H., Mahvi, A.H., Seyedsalehi, M., Jaafari, J., Hoseini, M., Safari, G.H., Dalvand, A., Aslani, H., Mirzaei, N., Ashrafi, S.D., 2017. Contamination and ecological risk assessment of heavy metals in street dust of Tehran, Iran. Int. J. Environ. Sci. Technol. 14, 2675–2682.

Kamani, H., Ashrafi, S.D., Isazadeh, S., Jaafari, J., Hoseini, M., Mostafapour, F.K., Bazrafshan, E., Nazmara, S., Mahvi, A.H., 2015. Heavy metal contamination in street dusts with various land uses in Zahedan, Iran. Bull. Environ. Contam. Toxicol. 94, 382–386.

Kara, M., 2020. Assessment of sources and pollution state of trace and toxic elements in street dust in a metropolitan city. Environ. Geochem. Health 42, 3213–3229.

Kargarfard, M., Shariat, A., Shaw, B.S., Shaw, I., Lam, E.T.C., Kheiri, A., Eatemadyboroujeni, A., Tamrin, S.B.M., 2015. Effects of polluted air on cardiovascular and hematological parameters after progressive maximal aerobic exercise. Lung 193, 275–281.

Khodadadi, N., Amini, A., Dehbandi, R., 2022. Contamination, probabilistic health risk assessment and quantitative source apportionment of potentially toxic metals (PTMs) in street dust of a highly developed city in north of Iran. Environ. Res. 210, 112962.

Khodeir, M., Shamy, M., Alghamdi, M., Zhong, M., Sun, H., Costa, M., Chen, L., Maciejczyk, P., 2012. Source apportionment and elemental composition of PM2.5 and PM10 in Jeddah city, Saudi Arabia. Atmos. Pollut. Res. 3, 331–340.

Kosheleva, N.E., Vlasov, D.V., Korlyakov, I.D., Kasimov, N.S., 2018. Contamination of urban soils with heavy metals in Moscow as affected by building development. Sci. Total Environ. 636, 854–863.

Kusin, F.M., Azani, N.N.M., Hasan, S.N.M.S., Sulong, N.A., 2018. Distribution of heavy metals and metalloid in surface sediments of heavily-mined area for bauxite ore in Pengerang, Malaysia and associated risk assessment. Catena 165, 454–464.

Latif, M.T., Yong, S.M., Saad, A., Mohamad, N., Baharudin, N.H., Mokhtar, M.B., Tahir, N.M., 2014. Composition of heavy metals in indoor dust and their possible exposure: a case study of preschool children in Malaysia. Air. Qual. Atmos Health 7, 181–193.

Li, N., Han, W., Tang, J., Bian, J., Sun, S., Song, T., 2018. Pollution characteristics and human health risks of elements in road dust in Changchun, China. Int. J. Environ. Res. Publ. Health 15, 1843.

Li, H.H., Chen, L.J., Yu, L., Guo, Z.B., Shan, C.Q., Lin, J.Q., Gu, Y.G., Yang, Z.B., Yang, Y.X., Shao, J.R., 2017. Pollution characteristics and risk assessment of human exposure to oral bioaccessibility of heavy metals via urban street dusts from different functional areas in Chengdu, China. Sci. Total Environ. 586, 1076–1084.

Li, H., Qian, X., Hu, W., Wang, Y., Gao, H., 2013. Chemical speciation and human health risk of trace metals in urban street dusts from a metropolitan city, Nanjing, SE China. Sci. Total Environ. 456, 212–221.

Li, X., Feng, L., Huang, C., Yan, X., Zhang, X., 2014. Chemical characteristics of atmospheric fallout in the south of Xi'an during the dust episodes of 2001–2012 (NW China). Atmos. Environ. 83, 109–118.

Lim, C.C., Thurston, G.D., Shamy, M., Alghamdi, M., Khoder, M., Mohorjy, A.M., Al Khalaf, A.K., Brocato, J., Chen, L.C., Costa, M., 2018. Temporal variation of fine and coarse particulate matter sources in Jeddah, Saudi Arabia. JAWMA 68, 123–138.

Long, Z., Zhu, H., Bing, H., Tian, X., Wang, Z., Wang, X., Wu, Y., 2021. Contamination, sources and health risk of heavy metals in soil and dust from different functional areas in an industrial city of Panzhihua City, Southwest China. J. Hazard Mater. 420, 126638.

Mazurek, R., Kowalska, J., Gąsiorek, M., Zadrozny, P., Jozefowska, A., Zaleski, T., Orłowska, K., 2017. Assessment of heavy metals contamination in surface layers of Roztocze National Park Forest soils (SE Poland) by indices of pollution. Chemosphere 168, 839–850.

McDonnell, W.F., Stewart, P.W., Smith, M.V., Kim, C.S., Schelegle, E.S., 2012. Prediction of lung function response for populations exposed to a wide range of ozone conditions. Inhal. Toxicol. 24, 619–633.

Mediolla, L., Domingues, M., Sandoval, M.G., 2008. Environmental assessment of and active tailings pile in the State of Mexico (central Mexico). Res. J. Environ. Sci. 2, 197–208.

Men, C., Liu, R., Xu, L., Wang, Q., Guo, L., Miao, Y., Shen, Z., 2020. Source-specific ecological risk analysis and critical source identification of heavy metals in road dust in Beijing China. J. Hazard Mater. 388, 121763.

Men, C., Liu, R., Xu, F., Wang, Q., Guo, L., Shen, Z., 2018. Pollution characteristics, risk assessment, and source apportionment of heavy metals in road dust in Beijing, China. Sci. Total Environ. 612, 138–147.

Mohammadi, A., Faraji, M., Conti, G.O., Ferrante, M., Miri, M., 2019. Mortality and morbidity due to exposure to particulate matter related to drying Urmia Lake in the NW Iran. Eur. J. Intern. Med. 60, e14–e15.

Mondal, S., Singh, G., Jain, M.K., 2020. Spatio-temporal variation of air pollutants around the coal mining areas of Jharia Coalfield, India. Environ. Monit. Assess. 192, 405.

Nematollahi, M.J., Dehdaran, S., Moore, F., Keshavarzi, B., 2021. Potentially toxic elements and polycyclic aromatic hydrocarbons in street dust of Yazd, a central capital city in Iran: contamination level, source identification, and ecological-health risk assessment. Environ. Geochem. Health 43, 485–519.

Neto, J.A.B., Gingele, F.X., Leipe, T., Brehme, I., 2006. Spatial distribution of heavy metals in surficial sediments from Guanabara Bay: rio de Janeiro, Brazil. Environ. Geol. 49, 1051–1063.

Ni, M., Mao, R., Jia, Z., Dong, R., Li, S., 2018. Heavy metals in soils of Hechuan County in the upper Yangtze (SW China): comparative pollution assessment using multiple indices with high-spatial-resolution sampling. Ecotoxiol. Environ. Saf. 148, 644–651.

Novo, L.A., Onishi, V.C., Bernardino, C.A., da Silva, E.F., 2017. Metal Bioaccumulation by Plants in Roadside Soils: Perspectives for Bioindication and Phytoremediation. Enhancing Cleanup of Environmental Pollutants. Springer, pp. 215–230.

Odediran, Et Adeniran, J.A., Yusuf, R.O., Abdulraheem, K.A., Adesina, O., Sonibare, J.A., Du, M., 2021. Contamination levels, health risks and source apportionment of potentially toxic elements in road dusts of a densely populated African City. Environ. Nanotechnol. Monit. Manag. 15, 100445.

Okedeyi, O.O., Dube, S., Awofolu, O., Nindi, M.M., 2014. Assessing the enrichment of heavy metals in surface soil and plant (Digitariaeriantha) around coal-fired power plants in South Africa. Environ. Sci. Pollut. Res. Int. 21, 4686–4696.

Osorio-Martinez, J., Silva, L.F., Flores, E.M., Nascimento, M.S., Picoloto, R.S., Olivero-Verbel, J., 2021. Environmental and human health risks associated with exposure to hazardous elements present in urban dust from Barranquilla, Colombian Caribbean. J. Environ. Qual. 50, 350–363.

Pan, H., Lu, X., Lei, K., 2017. A comprehensive analysis of heavy metals in urban road dust of Xi'an, China: contamination, source apportionment and spatial distribution. Sci. Total Environ. 609, 1361–1369.

Patel, D.K., Jain, M.K., 2022. Contamination and health risk assessment of potentially harmful elements associated with roadside dust in Dhanbad India. Stoch. Environ. Res. Risk Assess. 36, 389–407.

Perin, G., Craboledda, L., Lucchese, M., Cirillo, R., Dotta, L., 1985. Heavy metal speciation in the sediments of northern Adriatic Sea. A new approach for environmental toxicity determination. Heavy Met. Environ. 2, 454–456.

Pierson, W.E., 1989. Impact of air pollutants on athletic performance. Allergy Proc. 10, 209–214.

Pragg, C., Mohammed, F., 2019. Distribution and health risk assessment of heavy metals in road dust from an industrial estate in Trinidad, West Indies. Int. J. Environ. Health Res. 29, 1–8.

Qadeera, A., Saqib, Z.A., Xing, Z.A.C., Khalil, S.K., Usmanb, M., Huang, Y., Bashir, S., Ahmad, Z., Ahmed, S., Thebo, K.H., Liua, M., 2020. Concentrations, pollution indices and health risk assessment of heavy metals in road dust from two urbanized cities of Pakistan: comparing two sampling methods for heavy metals concentration. Sustain. Cities Soc. 53, 101959.

Rahman, Z., Singh, V.P., 2019. The relative impact of toxic heavy metals (THMs) (arsenic (As), cadmium (Cd), chromium (Cr)(VI), mercury (Hg), and lead (Pb)) on the total environment: an overview. Environ. Monit. Assess. 191, 419.

Resongles, E., Dietze, V., Green, D.C., Harrison, R.M., Ochoa-Gonzalez, R., Tremper, A. H., Weiss, D.J., 2021. Strong evidence for the continued contribution of lead deposited during the 20th Century to the atmospheric environment in London of today. Proc. Natl. Acad. Sci. USA 118, e2102791118.

Shabbaj II, Alghamdi, M.A., Shamy, M., Hassan, S.K., Alsharif, M.M., Khoder, M.I., 2018. Risk assessment and implication of human exposure to road dust heavy metals in Jeddah, Saudi Arabia. Int. J. Environ. Res. Publ. Health 15, 36.

Shahab, A., Zhang, H., Ullah, H., Rashid, A., Rad, S., Li, J., Xiao, H., 2020. Pollution characteristics and toxicity of potentially toxic elements in road dust of a tourist city, Guilin, China: ecological and health risk assessment. Environ. Pollut. 266, 115419.

Shaltout, A.A., Boman, J., Hassan, S.K., Abozied, A.M., Al Ashkar, E.A., Abd, Elkader, Oh, Yassin, M.A., Al Tamimi, J.H., 2020. Elemental composition of PM$_{2.5}$ aerosol in a residential–industrial area of a mediterranean megacity. Arch. Environ. Contam. Toxicol. 78, 68–78.

Shaltout, A.A., Hassan, S., Alomairy, S.E., Manousakas, M., Karydas, A.G., Eleftheriadis, K., 2019. Correlation between inorganic pollutants in the suspended particulate matter (SPM) and fine particulate matter (PM$_{2.5}$) collected from industrial and residential areas in Greater Cairo, Egypt. Air. Qual. Atmos Health 12, 241–250.

Siddiqui, A.U., Jain, M., Masto, R.E., 2020. Pollution evaluation, spatial distribution, and source apportionment of trace metals around coal mines soil: the case study of eastern India. Environ. Sci. Pollut. Res. 27, 10822–10834.

SPA. Saudi Press Agency, 2020. https://www.spa.gov.sa/viewstory.php?langar&new sid=2020503. (Accessed 12 June 2020) last accessed.

Srithawirat, T., Latif, M.T., 2015. Concentration of selected heavy metals in the surface dust of residential buildings in Phitsanulok. Thailand. Environ. Earth Sci. 74, 2701–2706.

Taiwo, A.M., Musa, M.O., Oguntoke, O., Afolabi, T.A., Sadiq, A.Y., Akanji, M.A., Shehu, M.R., 2020. Spatial distribution, pollution index, receptor modelling and health risk assessment of metals in road dust from Lagos metropolis, Southwestern Nigeria. Environ. Adv. 2, 100012.

Taylor, S.R., 1964. Abundance of chemical elements in the continental crust: a new table. Geochem. Cosmochim. Acta 28, 1273–1285.

Taylor, S.R., McLennan, S.M., 1985. The Continental Crust: its Composition and Evolution. Blackwell Scientific Publications, Oxford, UK.

Tiwari, A., 2022. Rethinking Streets: the Case of South Obhur. Jeddah. https://blogs.lse. ac.uk/mec/2022/01/12/rethinking-streets-the-case-of-south-obhur-jeddah/. (Accessed 4 February 2022) (last accessed.

Trujillo-Gonzalez, J.M., Torres-Mora, M.A., Keesstra, S., Brevik, E.C., Jimenez-Ballesta, R., 2016. Heavy metal accumulation related to population density in road dust samples taken from urban sites under different land uses. Sci. Total Environ. 553, 636–642.

USEPA, 2011. Exposure Factors Handbook Edition. EPA/600/R-09/052F. National Center for Environmental Assessment, Office of Research and Development, United States Environmental Protection Agency 20460, Washington, D.C.

USEPA, 2007. Method 6010C (SW-846): Inductively Coupled Plasma-Atomic Emission Spectrometry. Revision. http://www.cromlab.es/Articulos/Metodos/EPA/6000/6010c.pdf. (Accessed 4 February 2022) (last accessed.

USEPA, 2001. Supplemental Guidance for Developing Soil Screening Levels for Superfund Sites, OSWER 9355.4-24, Office of Solid Waste and Emergency Response. United States Environmental Protection Agency, Washington, DC, USA.

USEPA, 1993. Reference Dose (RfD): Description and Use in Health Risk Assessments, Background Document 1 A, Integrated Risk Information System (IRIS). United States Environmental Protection Agency, Washington, DC, USA.

USEPA, 1989. Risk Assessment Guidance for Superfund. In: Human Health Evaluation Manual (Part A), vol. I. United States Environmental Protection Agency, Washington, DC, USA. EPA/540/1-89/002, Office of Emergency and Remedial Response.

Vision, 2016. Saudi Arabia's Vision for 2030: Quality of Life Program. https://www.vision2030.gov.sa/v2030/vrps/qol/. (Accessed 4 February 2022) (last accessed.

Wang, H., Zhao, Y., Walker, T.R., Wang, Y., Luo, Q., Wu, H., Wang, X., 2021. Distribution characteristics, chemical speciation and human health risk assessment of metals in surface dust in Shenyang City, China. Appl. Geochem. 131, 105031.

Wang, H., Shen, C., Kang, Y., Deng, Q., Lin, X., 2020a. Spatial distribution of pollution characteristics and human health risk assessment of exposure to heavy elements in road dust from different functional areas of Zhengzhou. China. Environ. Sci. Pollut. Res. 27, 26650–26667.

Wang, X., Liu, E., Lin, Q., Liu, L., Yuan, H., Li, Z., 2020b. Occurrence, sources and health risks of toxic metal (loid)s in road dust from a mega city (Nanjing) in China. Environ. Pollut. 263, 114518.

Wang, S., Cai, L.M., Wen, H.H., Luo, J., Wang, Q.S., Liu, X., 2019. Spatial distribution and source apportionment of heavy metals in soil from a typical county-level city of Guangdong Province, China. Sci. Total Environ. 655, 92–101.

Yang, S., Liu, J., Bi, X., Ning, Y., Qiao, S., Yu, Q., Zhang, J., 2020. Risks related to heavy metal pollution in urban construction dust fall of fast developing Chinese cities. Ecotoxicol. Environ. Saf. 197, 110628.

Yi, Y., Yang, Z., Zhang, S., 2011. Ecological risk assessment of heavy metals in sediment and human health risk assessment of heavy metals in fishes in the middle and lower reaches of the Yangtze River basin. Environ. Pollut. 159, 2575–2585.

Yu, B., Lu, X., Fan, X., Fan, ., Zuo, L., Yang, Y., Wang, L., 2021. Analyzing environmental risk, source and spatial distribution of potentially toxic elements in dust of residential area in Xi`an urban area China. Ecotoxicol. Environ. Saf. 208, 111679.

Yuan, G.-L., Sun, T.-H., Han, P., Li, J., Lang, X.-X., 2014. Source identification and ecological risk assessment of heavy metals in topsoil using environmental geochemical mapping: typical urban renewal area in Beijing, China. J. Geochem. Explor. 136, 40–47.

Zhang, Y., Wu, D., Wang, C., Fu, X., Wu, G., 2020. Impact of coal power generation on the characteristics and risk of heavy metal pollution in nearby soil. Ecosys. Health Sustain. 6, 1–12.

Zhang, H., Mao, Z., Huang, K., Wang, X., Cheng, L., Zeng, L., Zeng, L., Zhou, Y., Jing, T., 2019. Multiple exposure pathways and health risk assessment of heavy metal(loid)s for children living in fourth- tier cities in Hubei Province. Environ. Int. 129, 517–524.

Zhao, G., Zhang, R., Han, Y., Meng, J., Qiao, Q., Li, H., 2021. Pollution characteristics, spatial distribution, and source identification of heavy metals in road dust in a central eastern city in China: a comprehensive survey. Environ. Monit. Assess. 193, 796.

Zhao, K., Fu, W., Qiu, Q., Ye, Z., Li, Y., Tunney, H., Qian, X., 2019. Spatial patterns of potentially hazardous metals in paddy soils in a typical electrical waste dismantling area and their pollution characteristics. Geoderma 337, 453–462.

Zheng, N., Liu, J., Wang, Q., Liang, Z., 2010. Health risk assessment of heavy metal exposure to street dust in the zinc smelting district, Northeast of China. Sci. Total Environ. 408, 726–733.